Holmium-Doped Sodium Zinc Molybdenum Tellurite Glasses

Jin-bao Chen
School of physics and electronic information
Yunnan normal university
Kunming, Yunnan, China
1441743141@qq.com

Ning Zhang
School of physics and electronic information
School of energy and environment science
Yunnan normal university
Kunming, Yunnan, China
miccozn@163.com

Shi-Qing Man*
School of physics and electronic information
School of energy and environment science
Yunnan normal university
Kunming, Yunnan, China
man_shiqing@yahoo.com

Abstract—We propose and demonstrate Sodium Zinc Molybdenum Tellurite glasses (Na_2O-ZnO-MoO_3-TeO_2 or NZMT) as suitable hosts for rare earth ion Holmium (Ho^{3+}) operating at 1.2μm and 1.37μm wavelength. The density, the refractive indices, the optical absorption have been measured. The Judd-Ofelt intensity parameters Ω_2, Ω_4, Ω_6, the radiative rates, the branching ratios, and the fluorescence lifetimes were calculated from Judd–Ofelt theory. Intense 1.2μm ($^5I_6 \rightarrow {}^5I_8$) and 1.37μm ($^5S_2, {}^5F_4 \rightarrow {}^5I_5$) emissions were observed in these glass systems under 539nm excitation. The bandwidth of the $^5I_6 \rightarrow {}^5I_8$ and $^5S_2, {}^5F_4 \rightarrow {}^5I_5$ transitions are ~60nm and 61nm , respectively. Measured fluorescence lifetimes of the $^5I_6 \rightarrow {}^5I_8$ (1.2μm) and $^5S_2, {}^5F_4 \rightarrow {}^5I_5$ (1.37 μm) decay at room temperature were 281μs and 43.5μs, respectively, and their quantum efficiencies were approximately 9.3% and 22%. From our data, it appears that Ho^{3+}-doped NZMT glasses are promising materials for waveguide lasers and amplifiers operation at 1.1-1.4μm wavelength range.

Keywords-Judd-Ofelt theory; Holmium; Tellurite; Optical Transitions

I. INTRODUCTION

Tellurite glasses combine the attributes of wide transmission region (0.35-6μm), good glass stability, rare-earth ion solubility, slow corrosion rate, lowest phonon energy spectrum among oxide glass formers, high refractive index, and high nonlinear refractive index[1]. Neodymium-doped tellurite singlemode fiber laser and Er^{3+}-doped tellurite singlemode fiber laser have been demonstrated recently[2,3]. The signal-gain characteristics of Er^{3+} doped tellurite fiber amplifiers are clarified based on spectroscopic properties and signal-gain measure-ments[4]. Among various rare earth ions, Ho^{3+} ion exhibits several electronic transitions in the visible and infrared regions. The Ho^{3+} doped optical materials are expected to demonstrate prominent emissions in IR region at around 1.20μm ($^5I_6 \rightarrow {}^5I_8$), 1.38μm (($^5F_4$, $^5S_2$)$\rightarrow {}^5I_5$), 1.46μm ($^5F_5 \rightarrow {}^5I_6$), and 1.65μm ($^5I_5 \rightarrow {}^5I_7$); and lasing action at 2.08μm ($^5I_7 \rightarrow {}^5I_8$) along with visible emissions at 0.54μm ($^5F_4, {}^5S_2 \rightarrow {}^5I_8$), 0.66μm ($^5F_5 \rightarrow {}^5I_8$), 0.75μm (($^5F_4, {}^5S_2$)$\rightarrow {}^5I_7$) regions.

Since the manufacturing process of silica glass fibers was significantly improved, reducing the attenuation caused by hydroxyl (OH^-) absorption to a promising degree of ~0.3dB/km[5], the wavelength region near the zero-dispersion of silica fibers at ~1.2μm may become a potential signal band to further enlarge the transmission capacity of the current optical networks.

Continuously increasing demand for data transmission capacity of optical communication systems has been stimulating an ongoing search for fiber optical amplifiers which operate within the low-loss transmission window of OH-free silica fiber (1.2-1.7μm) [5]. To completely exploit the second telecommunication window, however, both the short-wavelength edge (~1200nm) and E-(1360-1460nm) bands should be covered. Ho3+ shows promising to achieve some novel near-infrared emissions due to the rich multiple energy levels.

.In this paper, Ho^{3+} doped NZMT glasses suitable for 1.20μm and 1.37μm wavelength operation have been demonstrated. Absorption, emission, radiative lifetimes and non-radiative properties of the glasses were investigated.

II. EXPERIMENTS

Ho^{3+}-doped glasses were prepared from anhydrous sodium carbonate (Na_2CO_3), zinc oxide (ZnO), molybdenum oxide (MoO_3), and tellurium oxide (TeO_2) powders. All this powders (99.999-99.5% purity) were obtained from Strem Chemicals Company. The glasses samples used in this research have the following molar composition: $10Na_2O$-10ZnO-$10MoO_3$-$70TeO_2$. Ho^{3+}-

doped NZMT glasses were prepared by doping 1.0wt% Ho_2O_3 into the NZMT glass raw chemicals. The glass powders are melted in a platinum crucible by an electrically heated furnace at 750°C. The glasses were subsequently annealed at lower temperatures and then sliced and polished to dimensions of 20mm × 20mm × 2mm.

The density of this sample is 5.31g/cm^3. By using the Metricon 2010 prism coupler technique at three wavelengths the refractive indices were obtained. The NZMT glasses refractive indices were 1.950 and 2.011 at 633nm and 1550nm wavelength respectively.

Using Cary 5000 double-bean spectrophotometer the absorption spectra were obtained from 300nm to 2600nm. NIR fluorescence spectra as well as decay curves at 1.19μm ($^5I_6 \rightarrow {}^5I_8$, Ho^{3+}) and 1.36μm ($^5S_2, {}^5F_4 \rightarrow {}^5I_5$, Ho^{3+}) were recorded by an InSb detector (Edinburgh, FSP920C), a 539nm laser with a 4ns pulse width from an optical parametric oscillator (Opotek MagicPrism VIR) pumped by the 355nm line of a Nd:YAG laser was used as the pump source.

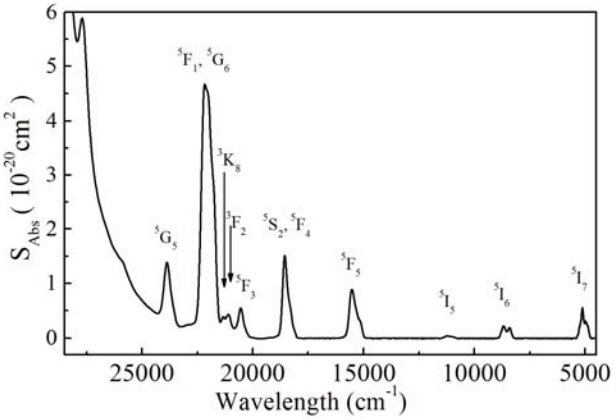

Figure 1. Absorption spectrum of Ho^{3+} doped NZMT glasses

III. RESULTS AND DISCUSSION

Fig. 1 shows the absorption spectrum of Ho^{3+}-doped NZMT glass. The absorption bands can be ascribed to transitions from the ground state ($^5I_8$) to the excited states of the Ho^{3+} ion. The band assignments are also indicated in this figure. The absorption spectra show wavelengths that may be used as pump lights for laser and optical amplifiers. Ten possible pump transitions are $^5I_8 \rightarrow {}^3G_5$ (419nm), $^5I_8 \rightarrow {}^5F_1, {}^5G_6$ (453nm), $^5I_8 \rightarrow {}^5F_2$ (474nm), $^5I_8 \rightarrow {}^3K_8$ (469nm) $^5I_8 \rightarrow {}^5F_3$ (487nm), $^5I_8 \rightarrow {}^5F_4, {}^5S_2$ (539nm), $^5I_8 \rightarrow {}^5F_5$ (644nm), $^5I_8 \rightarrow {}^5I_5$ (891nm), $^5I_8 \rightarrow {}^5I_6$ (1150nm), and $^5I_8 \rightarrow {}^5I_7$ (1952nm).

The radiative transition within the $4f^n$ configuration of a rare earth ion can be analyzed by using the Judd-Ofelt approach.[6,7] In the Judd-Ofelt theory, the electric-dipole transition line strength between two J states is expressed as[8]

$$S_{ed}(J;J') = \sum_{t=2,4,6} \Omega_t \left\langle \alpha SL, J \left\| U^{(t)} \right\| \alpha' S' L', J' \right\rangle^2, \quad (1)$$

where Ω_t are Judd-Ofelt parameter, J and J' specify the total angular momentum of initial and final states, αSL define all other quantum numbers needed to specify the states, and the $\langle \|U^{(t)}\| \rangle$ are double reduced matrix elements of unit tensor operators for the corresponding transition. It has been found that the matrix elements are essentially the same from host to host, and the matrix elements calculated by Weber et al. for Ho^{3+} in LaF_3 were used. [9]

The experimental oscillator strengths f_{exp} of the transitions are obtained by integrating absorption coefficients for each band using

$$f_{\exp} = \frac{2303mc^2}{N_A \pi e^2} \int \varepsilon(\nu) d\nu = 4.318 \times 10^{-9} \int \varepsilon(\nu) d\nu \quad (2)$$

where the quantities m and e are the mass and charge of the electron, c is the velocity of light, $\varepsilon(\nu)$ is the molar absorption coefficient, ν is the frequency, and N_A is the Avogadro's number. In principle, electric dipole transitions between f states are forbidden, as all these states have the same parity. But in practice the electronic states of the rare earth ions contain weak admixings of the 5d configuration and therefore the electric dipole oscillator strengths f_{ed} are typically in the order of 10^{-6}.[10] The magnetic dipole oscillator strengths f_{md} are much smaller for most transitions and in Ho^{3+} only the two transitions ($^5I_8 \rightarrow {}^5I_7$, $^5I_8 \rightarrow {}^3K_8$) are reported to contain significant magnetic contributions. The magnetic-dipole contributions, f_{md}, are obtained from the refractive indexes of the investigated glasses and the quantities, f', as reported in Ref.11.

$$f_{md} = nf', \quad (3)$$

For each wavelength, the refractive index was calculated using Cauchy's relation: $n=A+B/\lambda^2$, where A and B, for the tellurite glasses, are A=1.9092 and B=40870nm^2.

The relation between line strength S_{ed} and oscillator strength f for each electrical dipole transition is given by

$$f(J,J') = \frac{8\pi^2 mc(n^2+2)^2}{3h\bar{\lambda}(2J+1)9n} S_{ed}(J;J'), \quad (4)$$

where $\bar{\lambda}$ is the mean wavelength of the transition. Using the experimental oscillator strengths, the Judd-Ofelt intensity parameters Ω_t are determined by using a least-squares fitting approach. The measured and calculated oscillator strengths, the electric-dipole line strengths S_{ed} for some transitions, and the Judd-Ofelt intensity parameters of Ho^{3+} doped tellurite glasses are presented in Table. 1. A measure of the quality of the fit can be noted from the rms deviation δ_{rms} between the measured and calculated oscillator strengths as

$$\delta_{rms} = \left[\frac{\sum (\Delta f)^2}{N_{transition} - N_{parameter}}\right]^{1/2}, \quad (5)$$

TABLE I. THE MEASURED AND CALCULATED OSCILLATOR STRENGTHS, THE ELECTRIC-DIPOLE LINE STRENGTHS S_{ED} FOR SOME TRANSITIONS AND THE JUDD-OFELT INTENSITY PARAMETERS OF Ho^{3+} IN NZMT GLASSES

Transitions	Energy (cm^{-1})	f_{exp} (10^{-6})	f_{cal} (10^{-6})	f_{md} (10^{-6})	S_{ed}(10^{-6})
$^5I_8 \rightarrow {}^5I_7$	5124	2.2696	1.7313	0.5658	2.7850
$^5I_8 \rightarrow {}^5I_6$	8696	1.0338	1.2818		0.9792
$^5I_8 \rightarrow {}^5I_5$	11223	0.2073	0.2306		0.1495
$^5I_8 \rightarrow {}^5F_5$	15528	4.1440	3.9702		2.0779
$^5I_8 \rightarrow {}^5F_4, {}^5S_2$	18553	5.6281	5.1138		2.2802
$^5I_8 \rightarrow {}^5F_3$	20543	1.6739	1.5067		0.5965
$^5I_8 \rightarrow {}^5F_2$	21105	1.1595	0.9194		0.3990
$^5I_8 \rightarrow {}^3K_8$	21339	1.3036	1.2580	0.1336	0.4030
$^5I_8 \rightarrow {}^5F_1, {}^5G_6$	22057	30.6535	30.6111		9.9520
$^5I_8 \rightarrow {}^3G_5$	23866	4.3588	4.7596		1.2713
Ω_2 (10^{-20} cm^2)			4.95		
Ω_4 (10^{-20} cm^2)			2.61		
Ω_6 (10^{-20} cm^2)			1.55		
Root mean square deviation (10^{-6})			0.29		

where $\sum(\Delta f)^2$ is the sum of squares of deviations, $N_{transition}$ is the number of transitions, and $N_{parameter}$ is the number of parameters.

The measured and calculated oscillator strengths, the electric-dipole line strengths S_{ed} for some transitions, and the Judd-Ofelt intensity parameters of of Tm^{3+}-doped NZMT glasses are presented in Table 1. The Judd-Ofelt intensity parameters Ω_t, determined by using a least-squares fitting approach, are found to be $\Omega_2 = 4.95 \times 10^{-20}$ cm^2, $\Omega_4 = 2.61 \times 10^{-20}$ cm^2, and $\Omega_6 = 1.55 \times 10^{-20}$ cm^2. The rms deviation is 0.29×10^{-6}, which is comparable to the rms deviations found by applying the Judd-Ofelt theory to rare earth ions in other systems.

Using the Judd-Ofelt intensity parameters Ω_t some important radiative properties are calculated. The spontaneous transitions probability A is obtained using the equation[12]

$$A[(S,L)J:(S',L')J'] = \frac{64\pi^4 e^2 n}{3h(2J+1)\bar{\lambda}^3}\left[\frac{(n^2+2)^2}{9}\right] \times \sum_{t=2,4,6} \Omega_t \left\langle (S,L)J \left\| U^{(t)} \right\| (S',L')J' \right\rangle^2, \quad (6)$$

where h is Planck's constant, e is the charge of the electron, n is the refractive index, $\bar{\lambda}$ is the average wavelength of the transition, J is the total angular momentum of the initial state and the elements $<||U^{(t)}||>$ are the double reduced matrix elements of unit tensor operators calculated in the intermediate-coupling approximation.

The fluorescence branching ratio of transitions from initial manifold |(S,L)J> to lower levels |(S',L')J'> is given by

$$\beta[(S,L)J:(S',L')J'] = \frac{A[(S,L)J:(S',L')J']}{\sum_{S',L',J'} A[(S,L)J:(S',L')J']}, \quad (7)$$

and the peak stimulated emission cross section is calculated using

$$\sigma_{se} = \frac{\lambda^4}{8\pi c n^2}\frac{A}{\Delta\lambda_{eff}}, \quad (8)$$

where λ is peak fluorescence wavelength, $\Delta\lambda_{eff}$ is the effective fluorescence bandwidth and A is the spontaneous transition probability. The radiative lifetime is expressed as

$$\tau_R = \left\{ \sum_{S',L',J'} A[(S,L)J:(S',L')J'] \right\}^{-1} = A_{total}^{-1}. \quad (9)$$

Table. 2 gives the spontaneous transition probabilities A, the branching ratios β, and the calculated lifetimes τ_{rad} in Ho^{3+}-doped NZMT glasses.

Fig. 2 shows the emission spectra of Ho^{3+} doped NZMT glass in the range of 1080-1500 nm. Fluorescence bands at 1.2 μm ($^5I_6 \rightarrow {}^5I_8$) and 1.37 μm ($^5S_2, {}^5F_4 \rightarrow {}^5I_5$) were observed from the glass doped with 1.0 wt. % Ho_2O_3. The bandwidth of the $^5I_6 \rightarrow {}^5I_8$ and $^5S_2, {}^5F_4 \rightarrow {}^5I_5$ transitions are ~60 nm and 61nm , respectively.

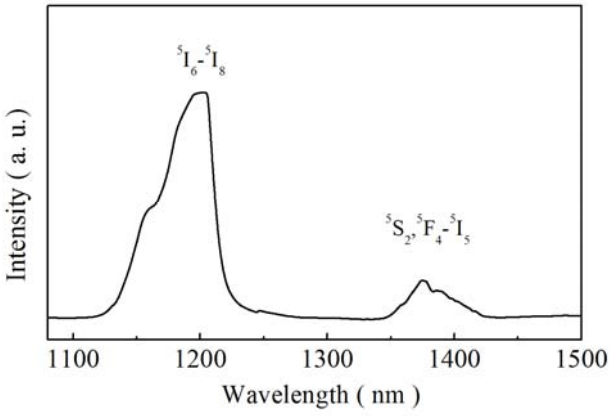

Figure 2. Absorption spectrum of Ho^{3+} doped NZMT glasses

TABLE II. PREDICTED SPONTANEOUS EMISSION PROBABILITIES OF OF Ho^{3+} IN NZMT GLASSES

Transitions	A_{ed} (s^{-1})	A_{md} (s^{-1})	A_{total} (s^{-1})	β_{ij}	τ_{rad} (μs)	τ_{meas} (μs)
$^5F_4 \rightarrow {}^5F_5$	20.84	5.53	26.37	0.0027	103	
$^5F_4 \rightarrow {}^5I_4$	38.20		38.20	0.0039		
$^5F_4 \rightarrow {}^5I_5$	260.58		260.58	0.0268		
$^5F_4 \rightarrow {}^5I_6$	629.10		629.10	0.0646		
$^5F_4 \rightarrow {}^5I_7$	885.06		885.06	0.0909		
$^5F_4 \rightarrow {}^5I_8$	7898.93		7898.93	0.8111		
$^5S_2 \rightarrow {}^5F_5$	0.92		0.92	0.0002	198	43.5
$^5S_2 \rightarrow {}^5I_4$	69.89		69.89	0.0139		
$^5S_2 \rightarrow {}^5I_5$	64.12		64.12	0.0127		
$^5S_2 \rightarrow {}^5I_6$	270.32		270.32	0.0536		
$^5S_2 \rightarrow {}^5I_7$	1712.25		1712.25	0.3397		
$^5S_2 \rightarrow {}^5I_8$	2923.60		2923.60	0.5800		
$^5F_5 \rightarrow {}^5I_4$	0.098		0.098	0.0000	200	
$^5F_5 \rightarrow {}^5I_5$	13.37		13.37	0.0027		
$^5F_5 \rightarrow {}^5I_6$	173.63		173.63	0.0347		
$^5F_5 \rightarrow {}^5I_7$	881.49		881.49	0.1763		
$^5F_5 \rightarrow {}^5I_8$	3930.41		3930.41	0.7862		
$^5I_4 \rightarrow {}^5I_5$	12.53	3.79	16.32	0.0884	5532	
$^5I_4 \rightarrow {}^5I_6$	70.01		70.01	0.3793		
$^5I_4 \rightarrow {}^5I_7$	81.02		81.02	0.4390		
$^5I_4 \rightarrow {}^5I_8$	17.22		17.22	0.0933		
$^5I_5 \rightarrow {}^5I_6$	14.26	7.95	22.21	0.0790	3658	
$^5I_5 \rightarrow {}^5I_7$	144.19		144.19	0.5126		
$^5I_5 \rightarrow {}^5I_8$	114.89		114.89	0.4084		
$^5I_6 \rightarrow {}^5I_7$	31.72	15.84	47.56	0.1367	3010	281
$^5I_6 \rightarrow {}^5I_8$	300.26		300.26	0.8633		
$^5I_7 \rightarrow {}^5I_8$	120.16	31.07	151.23	1.0000	8300	

Measured fluorescence lifetimes of the $^5I_6 \rightarrow {}^5I_8$ (1.2μm) and $^5S_2, {}^5F_4 \rightarrow {}^5I_5$ (1.37μm) decay at room temperature were 281μs and 43.5μs, respectively, and their quantum efficiencies were approximately 9.3% and 22%. From our data, it appears that Ho^{3+}-doped NZMT glasses are promising materials for use in lasers and optical amplifiers operating in the 1.1-1.40 μm wavelength range.

IV. CONCLUSIONS

The optical properties of Ho^{3+} doped NZMT glass are investigated. Intense 1.2 μm ($^5I_6 \rightarrow {}^5I_8$) and 1.37 μm ($^5S_2, {}^5F_4 \rightarrow {}^5I_5$) emissions were observed in these glass systems under 539-nm excitation. The bandwidth of the $^5I_6 \rightarrow {}^5I_8$ and $^5S_2, {}^5F_4 \rightarrow {}^5I_5$ transitions are ~60 nm and 61nm , respectively. Measured fluorescence lifetimes of the $^5I_6 \rightarrow {}^5I_8$ (1.2μm)and $^5S_2, {}^5F_4 \rightarrow {}^5I_5$ (1.37μm) decay at room temperature were 281μs and 43.5μs, respectively, and their quantum efficiencies were approximately 9.3% and 22%. Those results indicate that Ho^{3+} doped NZMT glass is a promising candidate for optical amplifier operation at 1.1-1.4 μm wavelength range.

ACKNOWLEDGMENT

This work is supported by the National Natural Science Foundation of China (NSFC) (Grant No. 21171072 and Grant No. 21361028).

REFERENCES

[1] J. S. Wang, E. M. Vogel and E. Snitzer, "Tellurite glass: a new candidate for fiber devices", Opt. Mat. **3**, 187 - 203 (1994).

[2] J. S. Wang, D. P. Machewirch, F. Wu, E. M. Vogel, and E. Snitzer, "Spectroscopic properties of neodymium-doped tellurite glass fiber ", Opt. Lett., **19**, 1448-1449 (1994).

[3] A. Mori, Y. Ohishi and S. Sudo, "Er^{3+} doped ultra-transparent oxy-fluoride glass-ceramics for application in the 1.54 μm telecommunication window", Electron. Lett.**, 33**, 863. (1997).

[4] Y. Ohishi, A. Mori, M. Yamada, H. Ono, Y. Nishida, and K. Oikawa, "Nonlinear optical properties of Er_2O_3-doped $75Nb_2O_5$-$20TeO_2$.5ZnO glasses", Opt. Lett., **23** 274 (1998).

[5] G. A. Thomas, B. I. Shraiman, P. F. Glodis, and M. J. Stephen, "Towards the clarity limit in optical fibre", Nature, **404**, 262–264 (2000).

[6] B.R. Judd, "Optical absorption intensities of rare-earth ions", Phys. Rev. **127**, 750-761 (1962).

[7] G. S. Ofelt, "Intensities of crystal spectra of rare-earth ions", J. Chem. Phys. **37**, 511-520 (1962).

[8] M. J. Weber, J. D. Myers and D. H. Blackburn, "Optical properties of Nd^{3+} in tellurite and phosphotellutite glasses." J. Appl. Phys. **52**, 2944-2949 (1981).

[9] M. J. Weber, B. H. Matsinger, V. L. Donlan, and G. T. Surratt, "Optical transition probabilities for trivalent holmium in LaF_3 and $YAlO_3$," J. Chem. Phys.**57**(1), 562–567 (1972).

[10] L. A. Riseberg, M. J. Weber, Progress in Optics vol.14, ch.3 p.89-159 (1976) North-Holland, Amsterdam.

[11] R. R. Jacobs and M. J.Weber, "Dependence of the $^4F_{3/2} \rightarrow {}^4I_{11/2}$ induced-emission cross section for Nd^{3+} on glass composition." IEEE J. Quantum Electron. QE-**12**, 102-111(1976).

[12] W. T. Carnall, P. R. Fields, K. Rajnak, “Radiative and non-radiative transitions of rare-earth ions in glasses”, J. Chem. Phys. **49**, 4412-4423 (1968).